Bulletin of Engineering Geology and the Environment
https://doi.org/10.1007/s10064-021-02284-5

ORIGINAL PAPER

Experimental investigations on the tensile behaviour of granite after heating and water-cooling treatment

Fan Zhang[1] · Cong Dai[1] · Yuhao Zhang[1,2] · Dianbin Guo[3] · Jianfu Shao[1,2] · Dawei Hu[4]

Received: 12 November 2020 / Accepted: 7 May 2021

Abstract

Thermal shock on tensile behaviour of granite is highly important for understanding of fracturing mechanism in hot dry rock. The effects of heating and water-cooling treatment (HWCT) on tensile behaviour of granite were investigated in this work. The granite samples were first heated to different predetermined temperatures and then rapidly cooled by water. The Brazilian split tests were carried out on the HWCT samples, and the strain gauges were used to measure the evolution of tensile deformation. With the increasing of heating temperature, the tensile stress–strain curves change from linear to non-linear, the axial tensile strain corresponding to failure point increases, and the tensile strength and tensile elastic modulus undergo a slight increase to decrease as the temperature increases. Finally, the mechanical properties under tensile condition were compared with those under compressive condition. Below 300 °C, the temperature has slight effect on both tensile and compressive strengths. Above 300 °C, the tensile properties decrease significantly after heating temperature threshold of 300 °C, while the heating temperature threshold for compressive properties is 500 °C. The thermal shock has a greater effect on tensile strength than on compressive strength.

Keywords Granite · High temperature · Heating and water-cooling treatment · Brazilian split test · Tensile behaviour

List of symbols

ε_3	Radial tensile strain
ε_1	Axial compressive strain
σ_t	Tensile strength of the sample
P	Peak force
D	Diameter of the sample
B	Thickness of the sample
E_t	Tensile elastic modulus
E_s	Splitting elastic modulus
L	Half length of the strain gauge
v	Poisson's ratio
E_T	Secant elastic modulus of the samples subjected to HWCT
σ_T	Peak strength of the samples subjected to HWCT
$E_{25°C}$	Secant elastic modulus of the initial samples
$\sigma_{25°C}$	Peak strength of the initial samples

✉ Fan Zhang
531606164@qq.com

[1] School of Civil Engineering, Architecture and Environment, Hubei University of Technology, Wuhan 430068, China

[2] LaMcube, University of Lille, CNRS, FRE2016, 59000 Lille, France

[3] Sinopec Star (Beijing) New Energy Research Institute Co., Ltd, Beijing 100083, China

[4] State Key Laboratory of Geomechanics and Geotechnical Engineering, Institute of Rock and Soil Mechanics, Chinese Academy of Sciences, Wuhan 430071, China

Introduction

Conventional energy resources such as oil and natural gas are gradually being depleted, and it is significant to seek for new clean energy sources to replace them. Hot dry rock (HDR) energy is a well-recognized clean and renewable green energy. HDR is widely distributed in granite with a depth of 2 to 6 km, and the temperature at that depth is generally 150 to 650 °C (Breede et al. 2013). The Enhanced Geothermal System (EGS) is considered to be an advanced and sustainable technology for heat extraction from HDR such as Fenton Hill in America (Jung 2013; Duchane and Brown 2002), Soultz-sous-Forêts in France (Genter et al. 2010; Tischner et al. 2007; Sausse and Genter 2005), and Ogachi in Japan (Ziagos et al. 2013). In the EGS, the well are drilled in high-temperature reservoirs, and cold water is then injected into the rock formation to fracture the formation

Published online: 28 May 2021

(Tran and Rahman 2007; Ueda et al. 2009; Bai et al. 2012; Zeng et al. 2013). Then, the cold water is absorbed by the rock formation and fractures; the heat energy is converted into hot fluid. Finally, the energy is converted by using the discharged water vapour or hot water to liquefy into liquid water to release thermal energy. Different from injection-induced tensile fractures in classical hydraulic fracturing, the thermal shock due to the large temperature difference between the cold water and hot rock formation could also result in fractures (Tang et al. 2020) and changes in mechanical properties (Siegesmund et al. 2000; Ruedrich et al. 2002; Brotons et al. 2014; Hashemi et al. 2015; Feng et al. 2018; Zhang et al. 2020a). Therefore, it is highly important to investigate the effect of thermal shock on the tensile behaviour of granites in EGS.

The effect of high temperature on the physical properties and mechanical behaviour of granites have been extensively investigated, and the results showed that heating treatment caused thermal fracture and consequently resulted in the variations of physical properties, i.e. porosity, wave velocity and permeability (Géraud et al. 1992; Chaki et al. 2008; Nasseri et al. 2009; Inserra et al. 2013; Guo et al. 2020; Zhao et al. 2020; Li et al. 2020c; Zhang et al. 2021). With the increase of heating temperature, the uniaxial compression strength (UCS) and elastic modulus usually undergo an increase–decrease transition for different granites, and the temperature threshold of the transition is different and related to the grain size and structure of granites (Chen et al. 2012; Zhang et al. 2014; Chen et al. 2017; Yang et al. 2017; Hu et al. 2018; Zhu et al. 2020a; Li et al. 2020a). The deterioration mechanisms of physical and mechanical behaviour of granite are mainly attributed to the generation and propagation of microcracks (Wang et al. 2020; Zhu et al. 2020b; Shen et al. 2020).

Alternatively, the effect of thermal shock (Zhang et al. 2018a, b; Fan et al. 2020), which is generally achieved by preheating to high temperatures, followed by rapid cooling in water, on the physical properties and mechanical behaviour of granites has been also investigated. Due to the relatively small thermal conductivity of granite, thermal shock could generate large temperature gradient and thermal damage inside materials and result in significant changes in porosity, permeability, wave velocity, bulk modulus and strength and even rock fragmentation under high heating temperature (Wong et al. 2017; Aversa and Evangelista 1998; Chaki et al. 2008; Liu and Xu 2014; Yin et al. 2015; Yu et al. 2015; Ozguven and Ozcelik 2014; Popov et al. 2016; Dobson et al. 2002; Vazquez et al. 2015; Yu et al. 2016; Zhang et al. 2018a, b; Fan et al. 2020; Zhang et al. 2020a, b). Further, the cooling rate during rapid cooling was also investigated by laboratory tests, and the results showed that thermal shock induced by rapid cooling can cause more damage to granite than that induced by slow cooling, which leads to a larger size and number of internal pores (Fan et al. 2020; Li et al. 2020b; Zhu et al. 2021).

The previous investigations mentioned above mainly focused on the effects of heating treatment or thermal shock on the mechanical properties of rocks obtained from uniaxial and triaxial compressive tests. However, the tensile and compressive mechanical properties of rocks are certainly different (Fellner and Supancic 2002; Dwivedi et al. 2008; Shao et al. 2014; Yin et al. 2015; Wu et al. 2019); the knowledge related to compressive properties cannot thus directly be applied to tensile properties. For this, the effects of thermal shock on the tensile mechanical behaviour of granite were investigated in this paper. A series of Brazilian split tests were conducted on the samples after the HWCT. The strain gauges were also used to measure the tensile deformation process. The variations in failure patterns tensile stress–strain curves, tensile strength and tensile elastic modulus due to thermal stock were discussed and compared with those under compressive condition. The test results could improve the knowledge of tensile mechanical behaviour of granite after thermal shock.

Test preparations

Preparations of granite samples

The granite samples used in the tests were collected from Chuanshanping Town, Hunan Province. The mineral compositions were analysed by the X-ray diffraction, and the results show that the main mineral components are feldspar, mica and quartz. The initial density, porosity and P-wave velocity are 2.66 g/cm^3, 0.98% and 5357 m/s respectively. The average tensile strength and uniaxial compressive strength of the initial granite samples are 10.2 and 138 MPa, respectively. The initial granite samples are grey-white, fresh and coarse-grained, with uniform texture, and no visible defects were observed on the rock surface. The diameter and length of the samples are 50 and 100 mm, respectively. The surface flatness of the samples is controlled within ± 0.2 mm, which satisfied the standards of the International Society of Rock Mechanics and Rock Engineering (ISRM) (Franklin et al. 1979). For each test condition, three same tests were performed, and their average value was used.

Heating and water-cooling treatment

The granite samples were first heated in a Muffle furnace TNX1200-30 at different pre-designed temperatures. The volume of the furnace is 12 L, with the maximum temperature measurement capacity of 1200 °C. The samples were evenly placed in the furnace chamber. A certain distance should be ensured between the samples to avoid the

influence of uneven heat caused by the contact between the samples and the chamber. The samples were heated in the furnace at atmospheric pressure with a rate of 5 °C/min, and this slow heating rate was used to avoid the generation of thermal gradient and to ensure that the cracking process was induced merely by the temperature effect (Zhang et al. 2018b, 2020a). After the pre-designed temperature was reached (e.g. 200, 300, 400, 500 and 600 °C), the heating temperature was held for 2 h to achieve the temperature stabilization throughout the samples (Zhang et al. 2018a). This temperature stabilization period is chosen according to the size and the thermal conductivity of the samples. A water-cooling treatment for 1 h was then performed by immersion of the samples into a container with a large volume of 25 L at 25 °C. Finally, the granite samples were kept in a desiccator at 105 °C during 24 h for the subsequent tests.

Scheme of Brazilian split test

In order to study the effect of HWCT on the tensile properties of granite, the Brazilian split tests were performed on the samples after HWCT. A schematic diagram of the Brazilian split test system is shown in Fig. 1a. The system has an axial force capacity of 1500 KN. A high-precision closed-loop servo-controlled system is used to control axial and hoop stress. In order to avoid stress concentration at the loading point, the arc fixture is selected (Fig. 1b). Two strain gauges were pasted to the centre positions of the two end faces of the sample along the radial and axial direction, respectively, and the radial tensile strain (ε_3), and axial compressive strain (ε_1) of the sample during the Brazilian split test was measured (see Fig. 1c). The sample was placed in the middle of the fixture, and the vertical compressive stress was applied under a strain-rate controlled mode at a rate of 0.01 mm/min. The mechanical parameters of the samples during the Brazilian split test were obtained. The tensile strength is

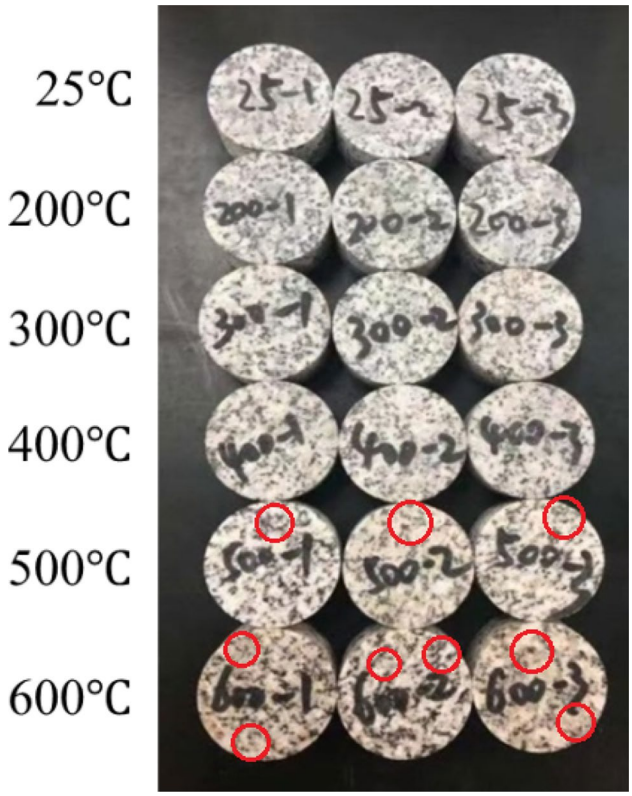

Fig. 2 Granite samples subjected to the thermal shock at different temperatures

calculated by the following formula (ISRM 1978) and the tensile stress–strain curve can be plotted:

$$\sigma_t = \frac{2P}{\pi DB} \tag{1}$$

where σ_t, P, D and B denote the tensile strength (MPa), peak force (N), diameter (mm) and thickness (mm) of the sample, respectively.

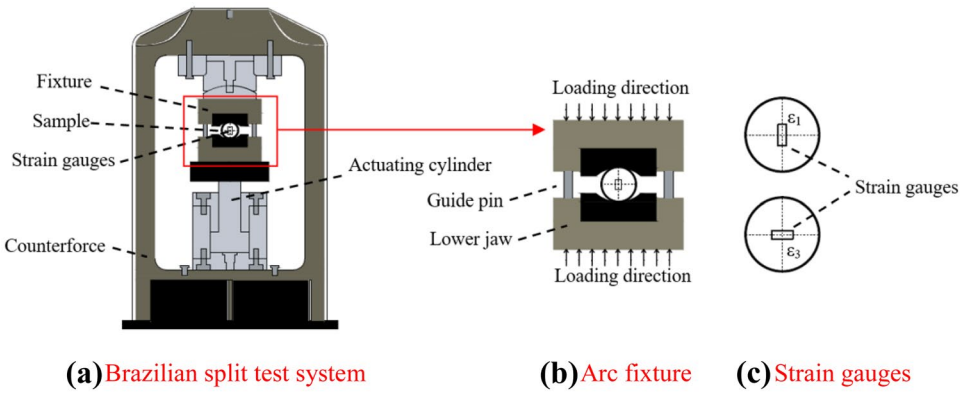

Fig. 1 Schematic diagram of Brazilian split test system: **a** Brazilian split test system, **b** arc fixture, **c** strain gauges

Test results

Variations in physical behaviour after HWCT

After the HWCT, the colour of the granite surface changes significantly (as shown in Fig. 2). It shows that as the temperature increases, the colour of the granite surface changes from grey-white to grey-red, which is caused by chemical changes within the rock (Li et al. 2017). When the heating temperature was higher than 500 °C, some yellow patches (as red circle shown in Fig. 2) appeared on the surface of the sample. When the temperature reached 600 °C, the surface of sample became loose and porous, but no obvious macro-cracks were observed. The similar phenomenon was also observed on other granites (Kumari et al. 2018; Fan et al. 2020).

Figure 3 presents the microcrack morphology of the initial sample and the samples after HWTC was obtained by scanning electron microscope (SEM), and the red dotted line indicates the microcracks. Few microcracks could be observed in the initial samples (Fig. 3a). After heating up to 200 °C and cooling to room temperature, a small number of microcracks could be found on weak interfaces of the crystals with the combining effect of heating and cooling treatment (Fig. 3b). With increasing temperature, the temperature differences between heating and cooling treatment increase, the number of microcracks increase gradually, the length and aperture of microcracks increase accordingly, some microcracks begin to connect together (Fig. 3c–e). When the heating temperature exceeds 500 °C (Fig. 3f), a large number of trans-granular cracks and cellular structures are observed

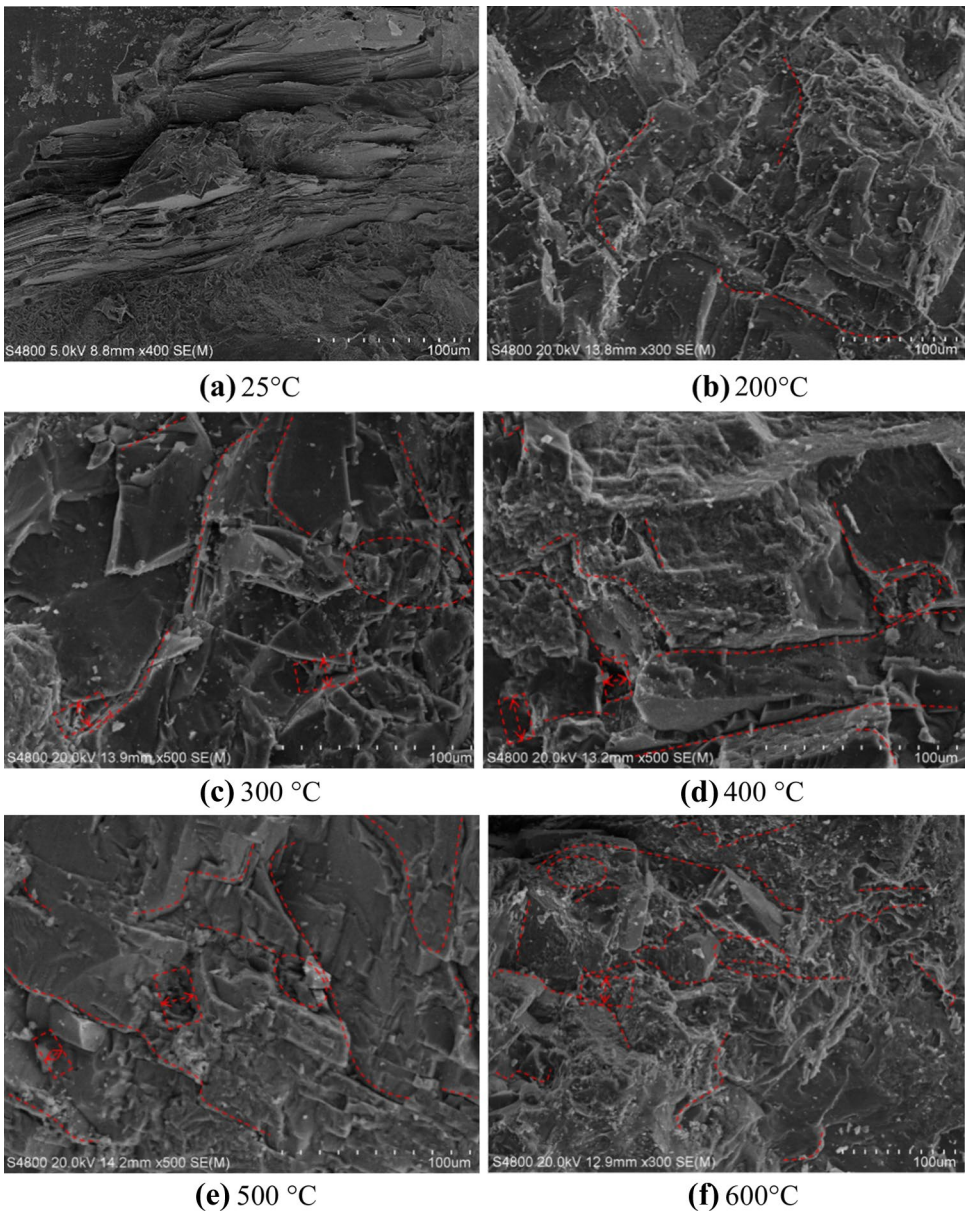

Fig. 3 Microcrack morphology due to HWCT at different heating temperatures: **a** 25 °C, **b** 200 °C, **c** 300 °C, **d** 400 °C, **e** 500 °C, **f** 600 °C

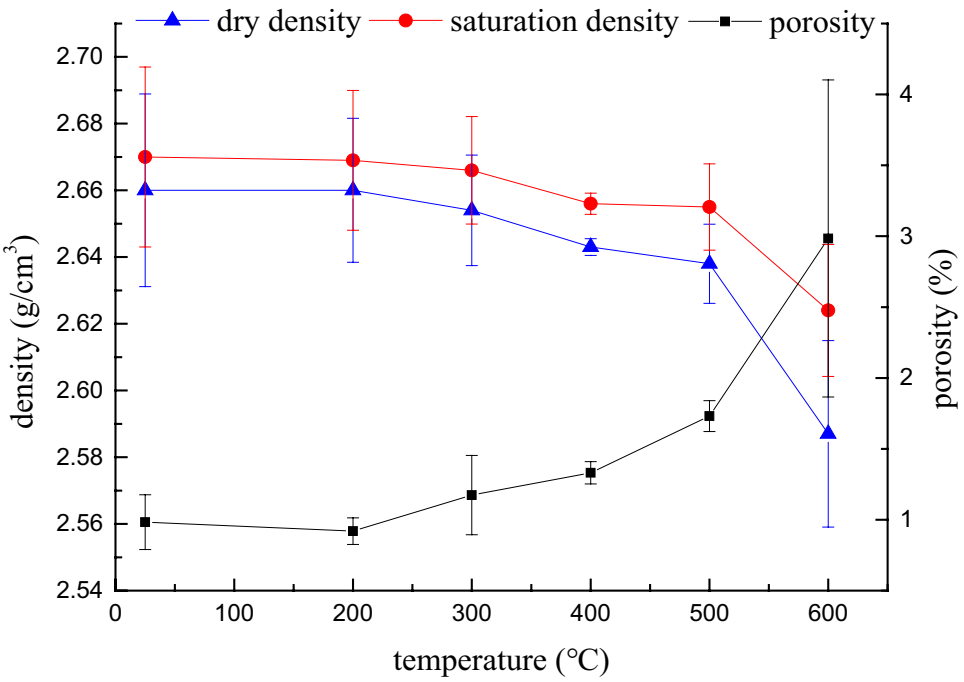

Fig. 4 Porosity and density variations after HWCT

due to the large temperature differences between heating and cooling treatment (Zhang et al. 2018a, b).

After the HWCT, the density, porosity and P-wave velocity of the granite samples were measured according to the recommended methods by the ISRM (Franklin et al. 1979). The variations of the density and the porosity after the HWCT with different heating temperatures are shown in Fig. 4. With increasing heating temperature, there is a continuous decrease in dry density and saturated density, while the porosity shows the inverse trend. From 25 to 500 °C, a slight increase in porosity is observed, and these minor structural modifications are attributed to the opening of initial microcracks and the nucleation of some new microcracks. Beyond 500 °C, the porosity showed a marked

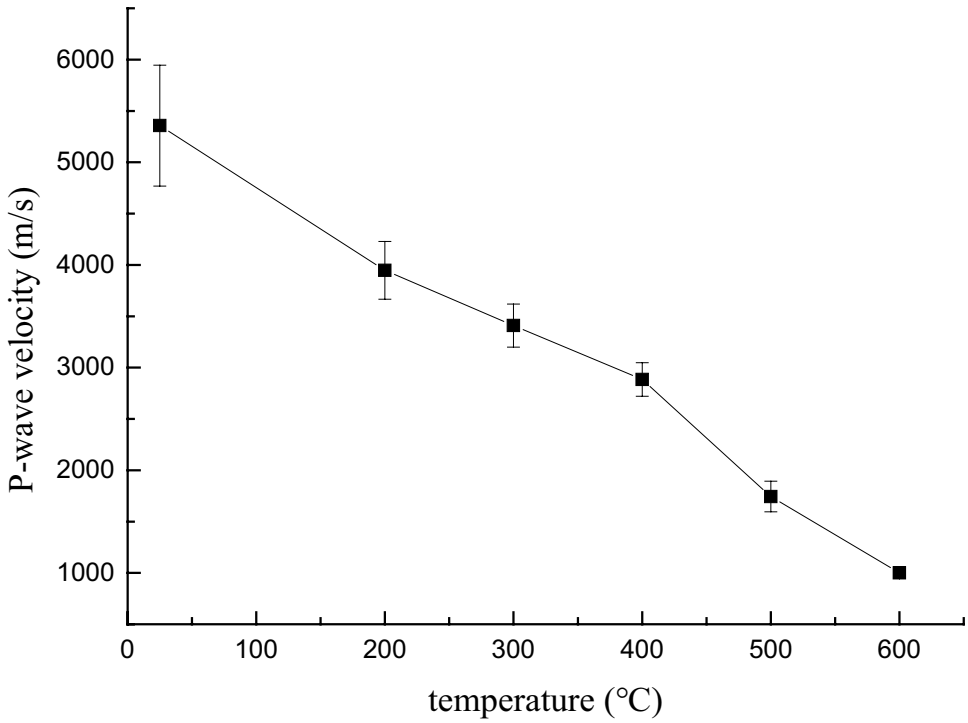

Fig. 5 P-wave velocity variations after HWCT

increase with heating temperature (from 1.731 to 2.984%), because quartz undergoes structural changes in crystals at 573 °C from α-type to β-type (Nasseri et al. 2009). Moreover, Fig. 5 presents a continuous decrease in P-wave velocity with increasing heating temperature, and the average value of P-wave velocity decreases significantly from 5357 m/s (25 °C) to 1000 m/s (600 °C). The decreased P-wave velocity is basically attributed to generation of microcracks due the combining effect of heating and cooling treatment.

Variations in tensile mechanical behaviour after HWCT

The typical stress–strain curves obtained from the Brazilian split tests are shown in Fig. 6. The tensile strain and compressive strain are measured by the strain gauges (Fig. 1c). Due to the strain gauges are split into two halves at the failure, the post-peak phase of the curves cannot be obtained for each heating temperature. When the heating temperature is between 25 and 400 °C, the tensile stress–strain curves are almost a straight line, few visible nonlinear phases could be observed, while a marked nonlinear phase occurs beyond 500 °C.

The failure patterns of the granite samples are shown in Fig. 7. It is found that the failure of all the samples occurred along the vertical loading direction, and the strain gauges pasted to the centre of the samples were split into two halves due to the generation of macrocrack. The difference of the failure patterns of the samples was not obvious with the increasing of heating temperature.

Discussions

Tensile elastic modulus and strength

The elastic modulus is a critical parameter related to rock deformation, and the tensile stress in practical engineering is often the key factor accounting for rock cracking. In this context, the tensile strain was measured by the strain gauges pasted to the centre of the sample. The calculation method of tensile elastic modulus proposed by Ye et al. (2009) is adopted:

$$E_{\mathrm{t}} = E_{\mathrm{s}}\left[\left(1 - \frac{D}{L}\arctan\frac{2L}{D}\right)(1-v) + \frac{2D^2(1+v)}{4L^2D^2}\right] \tag{2}$$

where E_t is the tensile elastic modulus (GPa), L is the half length of the strain gauge (mm), v is the Poisson's ratio; E_s is the splitting elastic modulus (GPa), which is the slope of the straight part of the tensile stress–strain curve in the Brazilian split test (40–60% of the peak strength; Yin et al. 2016). The variations in tensile elastic modulus of the samples after HWCT are shown in Fig. 8. The tensile elastic modulus undergoes a slight increase to decrease with the increases of heating temperature. More precisely, the tensile

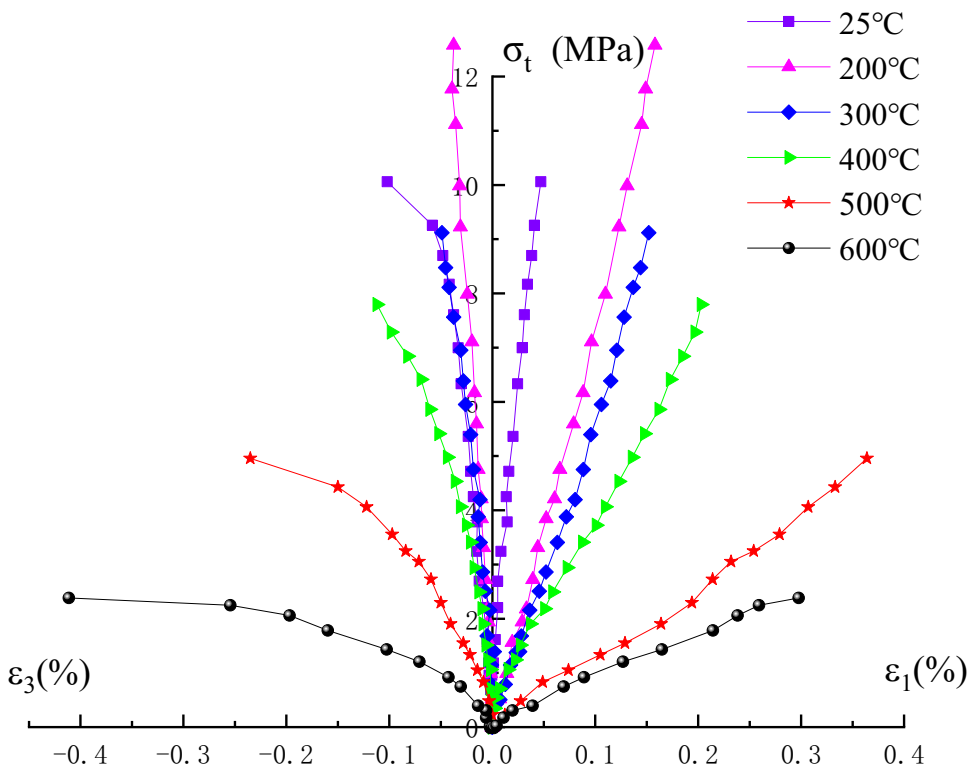

Fig. 6 The tensile stress–strain curves

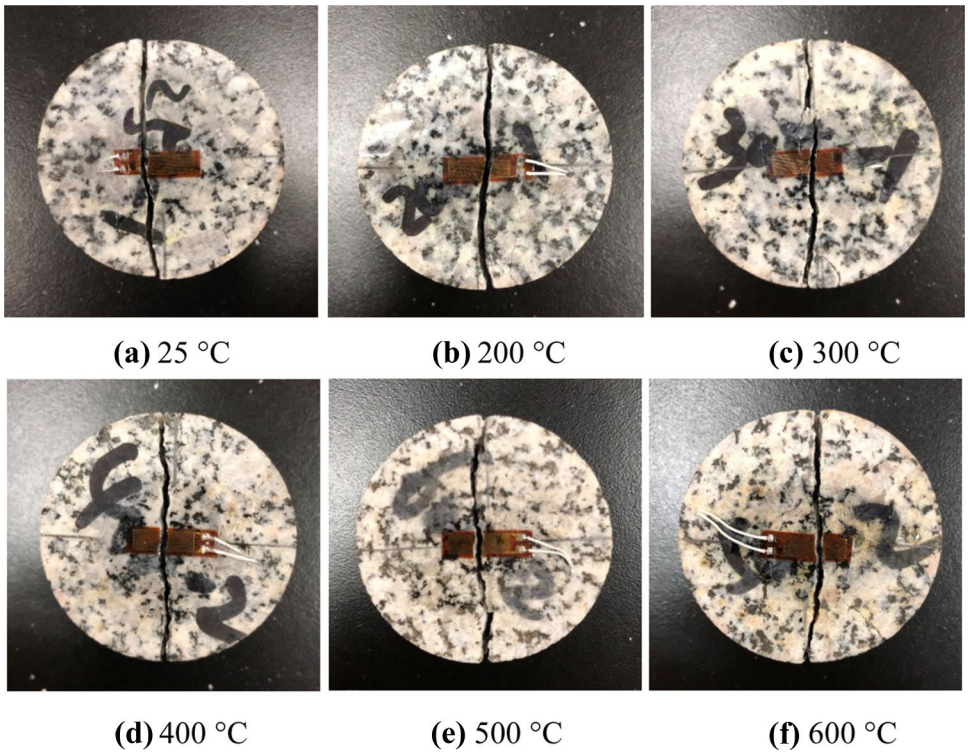

Fig. 7 Failure patterns of the granite samples in Brazilian split test: **a** 25 °C, **b** 200 °C, **c** 300 °C, **d** 400 °C, **e** 500 °C, **f** 600 °C

elastic modulus increases in the range of heating temperature between 25 and 200 °C, then decrease between 200 and 600 °C. Beyond 400 °C, the tensile elastic modulus decreases abruptly. The variations in tensile elastic modulus may be related to two types of competitive mechanism: thermal hardening and thermal shock induced cracking (Heap et al. 2017; Meredith and Atkinson 1985). When the granite samples were heated to a relatively low temperature, a thermal expansion was generated inside the samples and could cause a compaction effect on different crystal

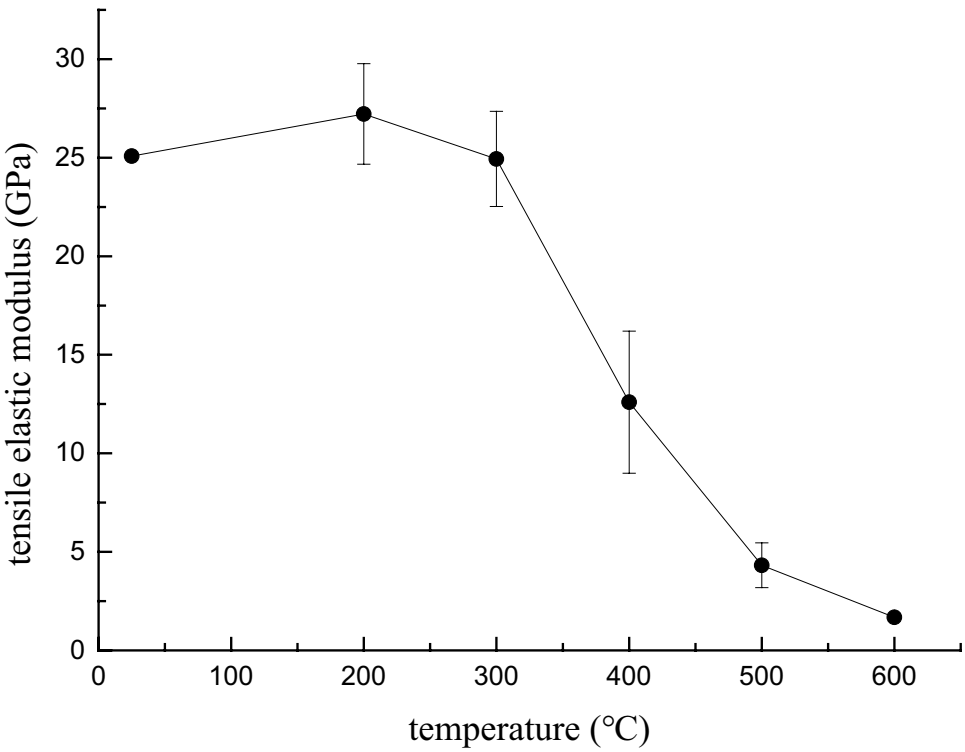

Fig. 8 Variations of tensile elastic modulus of granite samples after different HWCT

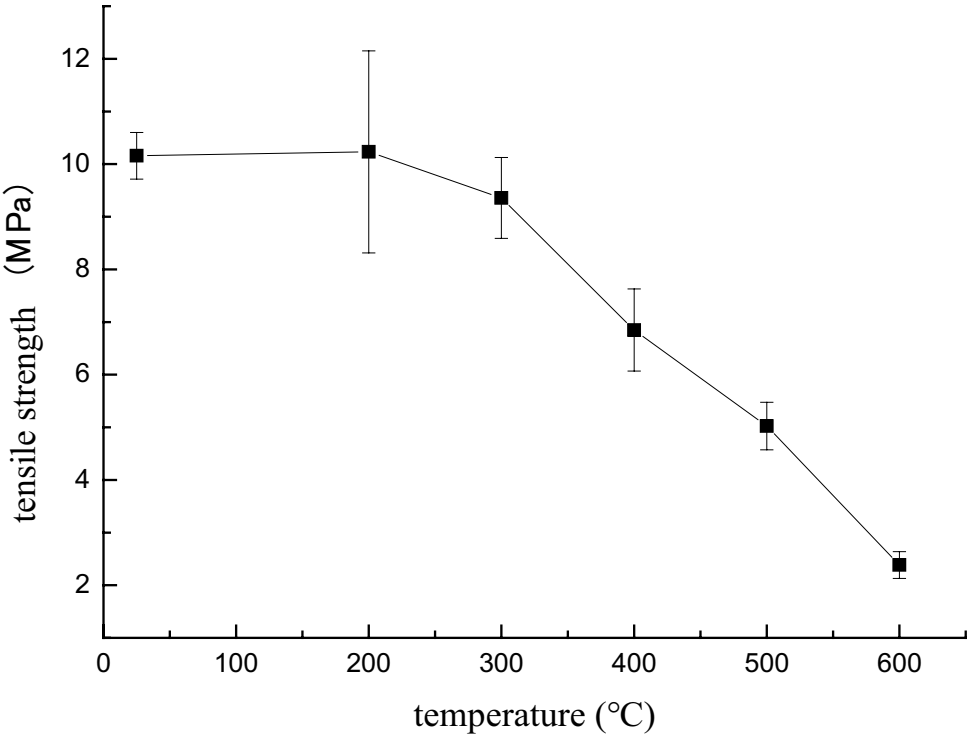

Fig. 9 Variations of tensile strength of granite samples after different HWCT

particles, which is considered as the origin of thermal hardening (Zhang et al. 2018b), leading to a slight increase in tensile elastic modulus. However, when the heating temperature is relatively high, the thermal shock during the rapid cooling process causes a strong temperature gradient, which is responsible for the generation of microcracks and consequently causes a decrease in tensile elastic modulus (Zhang et al. 2018a).

Figure 9 presents the tensile strength variations of the samples after HWCT. A transition of a slight increase to decrease with the increase of heating temperature is also observed on the tensile strength. The tensile strength of the granite samples at room temperature is 10.2 MPa. While the tensile strength is 2.38 MPa when the heating temperature is 600 °C, which was one-fifth of that at room temperature. Moreover, the tensile strength is observed to decrease slower between 200 and 300 °C rather than between 400 and 600 °C. In other words, there is a change in the decrease rate of tensile strength around 400 °C, which confirms the evolution of the tensile modulus. This transition in the tensile strength is also attributed to the thermal hardening at relatively low temperature and thermal shock–induced cracking at high temperature (Zhang et al. 2018b, 2020a).

Comparisons of tensile and compressive mechanical behaviour

The effect of HWCT treatment on tensile elastic modulus may be related to two types of competitive mechanism: thermal hardening and thermal shock during the heating and cooling process, and the latter one can cause thermal cracks inside the granite samples when the temperature difference is relatively large. Those microcracks will affect the tensile and compressive mechanical behaviour of granite (Zhang et al. 2018b, 2020b). In order to compare the effects of HWCT on compressive and tensile mechanical behaviour, uniaxial compression tests were also performed on the same granite subjected to HWCT. For the sake of clear comparison, the normalized elastic modulus ($\frac{E_T}{E_{25°C}}$)and peak strength ($\frac{\sigma_T}{\sigma_{25°C}}$) are used. E_T and σ_T, respectively, denote the secant elastic modulus (GPa) and peak strength (MPa) of the samples subjected to HWCT (T = 25, 200, 300, 400 and 600 °C). $E_{25°C}$ and, $\sigma_{25°C}$ respectively, denote the secant elastic modulus (GPa) and peak strength (MPa) of the initial samples. The normalized variation curves with the heating temperature of elastic modulus and peak strength in the compressive and tensile tests are plotted in Figs. 10 and 11. The variation trends in strength and elastic modulus are basically consistent for both uniaxial compression tests and Brazilian split tests. The transition of slight increase to decrease with the increase of the heating temperature is observed in both elastic modulus and strength in the two cases. When the heating temperature is 200 °C, the slight increases in the elastic modulus and strength are not obvious. This phenomenon indicates that the effects of thermal hardening on the tensile and compressive properties are slight at low heating temperature in a global sense. Moreover, the decreasing rate in the tensile properties is observed to be significantly larger

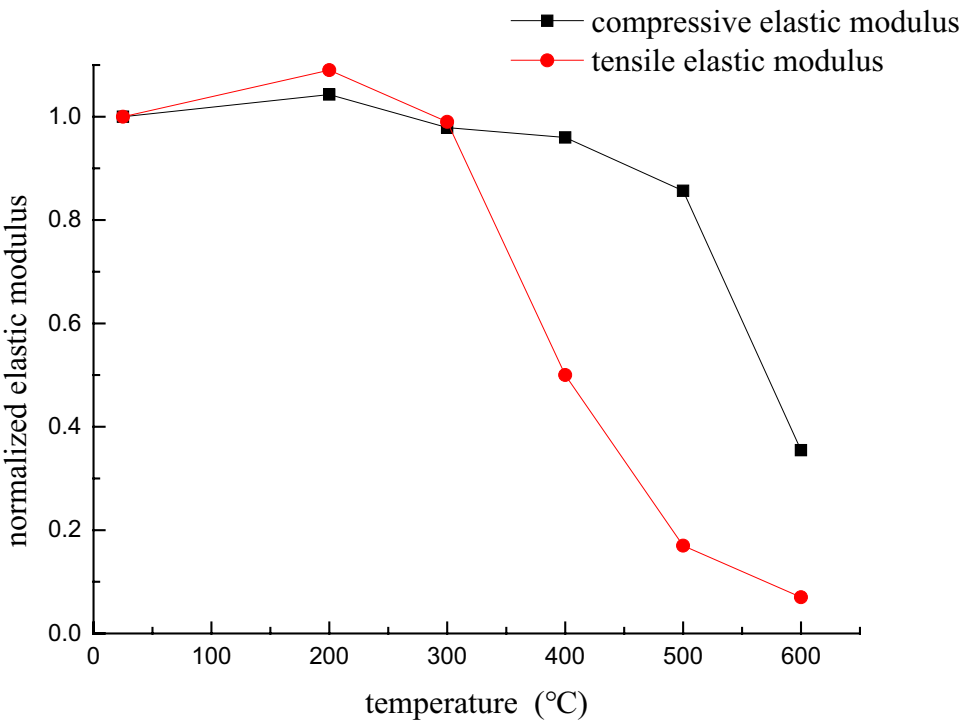

Fig. 10 Variations of normalized tensile and compressive elastic modulus with heating temperature

rather than in the compressive properties, and the tensile strength is significantly reduced when the heating temperature is between 300 and 400 °C, while it is between 500 and 600 °C for the compressive strength. Thermal shock–induced cracking at high temperature reduces the cohesion of granite and weakened the tensile strength of the granite, while it has a relatively small impact on the compressive strength of the granite. Between 500 and 600 °C, the compressive and tensile properties decrease sharply, indicating that the internal structure of granite is significantly damaged at 600 °C.

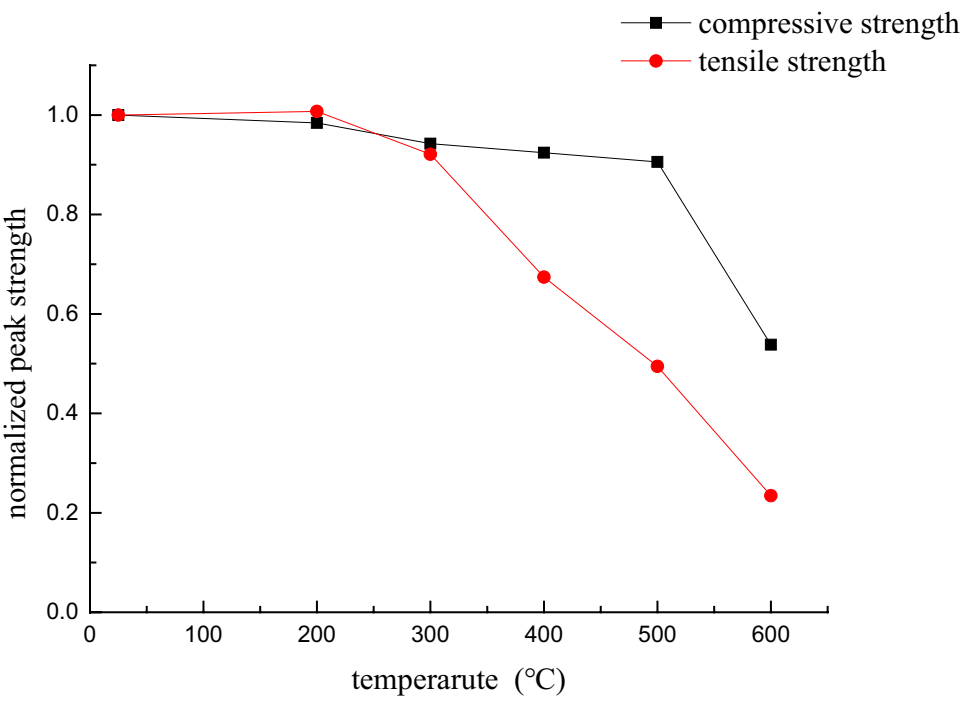

Fig. 11 Variations of normalized tensile and compressive strength with heating temperature

In the Brazilian split tests, the stresses along loading and vertical loading directions at the edge of fixture, where the clamp contacts the disc, are both compressive stresses. As the position moved toward the centre of the disc, the compressive stress in the loading direction gradually decreases and tensile stress appears. As the axial force increases, the axial compressive stress and the radial tensile stress increase gradually. If the thermal shock induced microcracks appear in the centre of the disc, under the action of radial tensile stress, the microcracks will rapidly expand and penetrate other microcracks, which results in extending of macrocracks to both ends. However, during the uniaxial compression process of granite, the thermal shock–induced microcracks would be closed under compressive stress. Therefore, the HWCT has a relatively smaller impact on compressive properties rather than on tensile properties.

Further, the different effects of HWCT on the tensile and compressive mechanical behaviour could also be related to the microcrack morphology (see Fig. 2) from the microscopic viewpoint. As the heating temperature increases, the temperature difference during thermal shock is consequently increased, the number of microcracks on the weak interface of the mineral increases after thermal shock, the length and pore size increase, and some coalescence of the microcracks are even observed (see Fig. 2e, f). The ability of granite to resist damage depends on the strength of the skeleton, the size of internal cracks and the strength and cohesion of the mineral composition (Zhao 2015; Liu et al. 2019; Kumari et al. 2019). The main factors affecting the tensile behaviour of granite are the cohesion and fracture state of mineral particles under tensile test (Gautam et al. 2018; Qi et al. 2020). On the other hand, the main factor affecting the compressive behaviour of granite is the properties of the interface between mineral particles (Li et al. 2013; Sun et al. 2015). The resistance to overcome and the main influencing factors are different, and the variation of tensile behaviour and compressive behaviour affected by temperature is also different. It indicates that the HWCT has different effects on tensile and compressive mechanical behaviour. When the heating temperature is between 300 and 400 °C, the increase and development of thermal shock–induced microcracks cause the decrease of tensile properties, while the compressive behaviour of granite does not significantly decrease, indicating that the threshold temperature of tensile is not enough to affect the internal structural framework of granite. When the temperature reaches 600 °C, the quartz undergoes a phase transition leading to the increasing of volume and generation of a large number of microcracks (Nasseri et al. 2009; Glover et al. 1995; Zhang et al. 2016; Wang et al. 2020). It causes the internal pores to increase and the extension and development of new microcracks, which leads to the fracture of the internal mechanical structure of the granite and the significant deterioration of the compressive mechanical properties.

Conclusions

The effects of HWCT on the physical and tensile mechanical properties were studied in this paper. As the temperature increases, the axial tensile strain of granite increases gradually, the tensile stress–strain curves change from linear to nonlinear, and the nonlinear characteristic increases with increasing temperature. The transition of slight increase to decrease with the increasing of heating temperature is observed in both tensile elastic modulus and tensile strength. Moreover, the uniaxial compression tests were also performed on the same granite subjected to HWCT to compare the effects of HWCT on compressive and tensile mechanical behaviour. The HWCT has different effects on tensile and compressive mechanical behaviour, and the tensile properties of granite decrease significantly after heating temperature threshold of 300 °C, while the heating temperature threshold for compressive properties is 500 °C. The thermal shock–induced microcracks are more prone to extension under tensile stress rather than under compressive stress; consequently, the HWCT has a relatively larger impact on tensile properties rather than on compressive properties.

Funding This work was jointly supported by the National Key Research and Development Program of China (Nos. 2018YFC0809600, 2018YFC0809601) and the Natural Science Foundation of China (grant numbers 51979100 and 51779252).

References

Aversa S, Evangelista A (1998) The mechanical behaviour of a pyroclastic rock: yield strength and "destructuration" effects. Rock Mech Rock Eng 31(1):25–42. https://doi.org/10.1007/s006030050007

Bai M, Reinicke KM, Teodoriu C et al (2012) Investigation on water–rock interaction under geothermal hot dry rock conditions with a novel testing method. J Pet Sci Eng 90–91:26–30. https://doi.org/10.1016/j.petrol.2012.04.009

Breede K, Dzebisashvili K, Liu XL et al (2013) A systematic review of enhanced (or engineered) geothermal systems: past, present and future. Geotherm Energy 1:4. https://doi.org/10.1186/2195-9706-1-4

Brotons V, Tomas R, Ivorra S et al (2014) Relationship between static and dynamic elastic modulus of calcarenite heated at different temperatures: the San Julián's stone. Bull Eng Geol Environ 73(3):791–799. https://doi.org/10.1007/s10064-014-0583-y

Chaki S, Takarli M, Agbodjan WP (2008) Influence of thermal damage on physical properties of a granite rock: porosity, permeability and ultrasonic wave evolution. Constr Build Mater 22(7):1456–1461. https://doi.org/10.1016/j.conbuildmat.2007.04.002

Chen SW, Yang CH, Wang GB (2017) Evolution of thermal damage and permeability of Beishan granite. Appl Therm Eng 110:1533–1542. https://doi.org/10.1016/j.applthermaleng.2016.09.075

Chen YL, Ni J, Shao W et al (2012) Experimental study on the influence of temperature on the mechanical properties of granite under uni-axial compression and fatigue loading. Int J Rock Mech Min Sci 56:62–66. https://doi.org/10.1016/j.ijrmms.2012.07.026

Dobson DP, Meredith PG, Boon SA (2002) Simulation of subduction zone seismicity by dehydration of serpentine. Science 298(5597):1407–1410. https://doi.org/10.1126/science.1075390

Duchane D, Brown D (2002) Hot dry rock (HDR) geothermal energy research and development at Fenton Hill, New Mexico. Geo-Heat Centre Quarterly Bulletin 23:13–19

Dwivedi RD, Goela RK, Prasada VVR et al (2008) Thermo-mechanical properties of Indian and other granites. Int J Rock Mech Min Sci 45(3):303–315. https://doi.org/10.1016/j.ijrmms.2007.05.008

Fan LF, Gao JW, Du XL et al (2020) Spatial gradient distributions of thermal shock-induced damage to granite. J Rock Mech Geotech Eng. https://doi.org/10.1016/j.jrmge.2020.05.004

Fellner M, Supancic P (2002) Thermal shock failure of brittle materials. Key Eng Mater 223:97–106. https://doi.org/10.4028/www.scientific.net/KEM.223.97

Feng ZJ, Zhao YS, Zhang Y et al (2018) Real-time permeability evolution of thermally cracked granite at triaxial stresses. Appl Therm Eng 133:194–200. https://doi.org/10.1016/j.applthermaleng.2018.01.037

Franklin JA, Vogler UW, Szlavin J (1979) Suggested methods for determining water content, porosity, density, absorption and related properties and swelling and slake-durability index properties: part 1: suggested methods for determining water content, porosity, density, absorption and related properties. Int J Rock Mech Min Sci Geomech Abstr 16:143–151. https://doi.org/10.1016/0148-9062(79)91452-9

Gautam PK, Verma AK, Jha MK et al (2018) Effect of high temperature on physical and mechanical properties of Jalore granite. J Appl Geophys 159:460–474. https://doi.org/10.1016/j.jappgeo.2018.07.018

Genter A, Goerke X, Graff J-J et al (2010) Current status of the EGS Soultz geothermal project (France). In: world geothermal congress, WGC2010, Bali, Indonesia pp 25–29

Géraud Y, Mazerolle F, Raynaud S (1992) Comparison between connected and overall porosity of thermally stressed granites. J Struct Geol 14(8–9):981–990. https://doi.org/10.1016/0191-8141(92)90029-V

Glover P, Baud P, Darot M et al (1995) α/β phase transition in quartz monitored using acoustic emissions. Geophys J Int 120:775–782. https://doi.org/10.1111/j.1365-246X.1995.tb01852.x

Guo YD, Huang LQ, Li XB et al (2020) Experimental investigation on the effects of thermal treatment on the physical and mechanical properties of shale. J Nat Gas Sci Eng 82:103496. https://doi.org/10.1016/j.jngse.2020.103496

Hashemi SS, Melkoumian N, Taheri A (2015) A borehole stability study by newly designed laboratory tests on thick-walled hollow cylinders. J Rock Mech Geotech Eng 7(5):519–531. https://doi.org/10.1016/j.jrmge.2015.06.005

Heap MJ, Violay M, Wadsworth FB et al (2017) From rock to magma and back again: the evolution of temperature and deformation mechanism in conduit margin zones. Earth Planet Sci Lett 463:92–100. https://doi.org/10.1016/j.epsl.2017.01.021

Hu JJ, Sun Q, Pan XH (2018) Variation of mechanical properties of granite after high-temperature treatment. Arab J Geosci 11(2):43. https://doi.org/10.1007/s12517-018-3395-8

Inserra C, Biwa S Chen YQ (2013) Influence of thermal damage on linear and nonlinear acoustic properties of granite. Int J Rock Mech Min Sci 62:96–104. https://doi.org/10.1016/j.ijrmms.2013.05.001

ISRM (1978) Suggested methods for determining tensile-strength of rock materials. Int J Rock Mech Min Sci 15(3):99–103. https://doi.org/10.1016/0148-9062(78)90003-7

Jung R (2013) EGS — goodbye or back to the future 95. In: Effective and Sustainable Hydraulic Fracturing. https://doi.org/10.5772/56458

Kumari WGP, Beaumont DM, Ranjith PG et al (2019) An experimental study on tensile characteristics of granite rocks exposed to different high-temperature treatments. Geomech Geophys Geo-Energ Geo-Resour 5(1):47–64. https://doi.org/10.1007/s40948-018-0098-2

Kumari WGP, Ranjith PG, Perera MSA et al (2018) Experimental investigation of quenching effect on mechanical, microstructural and flow characteristics of reservoir rocks: thermal stimulation method for geothermal energy extraction. J Pet Sci Eng 162:419–433. https://doi.org/10.1016/j.petrol.2017.12.033

Li N, Ma XF, Zhang SC et al (2020a) Thermal effects on the physical and mechanical properties and fracture initiation of Laizhou granite during hydraulic fracturing. Rock Mech Rock Eng 53(6):2539–2556. https://doi.org/10.1007/s00603-020-02082-7

Li X, Li BJ, Li XB et al (2020b) Thermal shock effects on the mechanical behavior of granite exposed to dynamic loading. Arch Civ Mech Eng 20:1–11. https://doi.org/10.1007/s43452-020-00070-w

Li Y, Yu HF, Zheng LN et al (2013) Compressive strength of fly ash magnesium oxychloride cement containing granite wastes. Constr Build Mater 38:1–7. https://doi.org/10.1016/j.conbuildmat.2012.06.016

Li YB, Zhai Y, Wang CS et al (2020c) Mechanical properties of Beishan granite under complex dynamic loads after thermal treatment. Eng Geol 267:105481. https://doi.org/10.1016/j.enggeo.2020.105481

Li ZH, Wong LNY, Teh CI (2017) Low cost colorimetry for assessment of fire damage in rock. Eng Geol 228:50–60. https://doi.org/10.1016/j.enggeo.2017.07.006

Liu S, Xu JY (2014) Mechanical properties of Qinling biotite granite after high temperature treatment. Int J Rock Mech Min Sci 71:188–193. https://doi.org/10.1016/j.ijrmms.2014.07.008

Liu ZB, Zhou HY, Zhang W et al (2019) A new experimental method for tensile property study of quartz sandstone under confining pressure. Int J Rock Mech Min Sci 123:104091. https://doi.org/10.1016/j.ijrmms.2019.104091

Meredith PG, Atkinson BK (1985) Fracture toughness and subcritical crack growth during high-temperature tensile deformation of Westerly granite and Black gabbro. Phys Earth Planet Inter 39(1):33–51. https://doi.org/10.1016/0031-9201(85)90113-X

Nasseri MHB, Tatone BSA, Grasselli G et al (2009) Fracture toughness and fracture roughness interrelationship in thermally treated westerly granite. Pure Appl Geophys 166(5–7):801–822. https://doi.org/10.1007/s00024-009-0476-3

Ozguven A, Ozcelik Y (2014) Effects of high temperature on physico-mechanical properties of Turkish natural building stones. Eng Geol 183:127–136. https://doi.org/10.1016/j.enggeo.2014.10.006

Popov Y, Beardsmore G, Clauser C et al (2016) ISRM suggested methods for determining thermal properties of rocks from laboratory tests at atmospheric pressure. Rock Mech Rock Eng 49(10):4179–4207. https://doi.org/10.1007/s00603-016-1070-5

Qi SW, Lan HX, Martin D, Huang XL (2020) Factors controlling the difference in brazilian and direct tensile strengths of the Lac du Bonnet Granite. Rock Mech Rock Eng 53:1005–1019. https://doi.org/10.1007/s00603-019-01946-x

Ruedrich J, Weiss T, Siegesmund S et al (2002) Thermal behaviour of weathered and consolidated marbles. Geol Soc Lond Spec Publ 205(1):255–271. https://doi.org/10.1144/GSL.SP.2002.205.01.19

Sausse J, Genter A (2005) Types of permeable fractures in granite. Geol Soc Lond Spec Publ 240:1–14. https://doi.org/10.1144/GSL.SP.2005.240.01.01

Shao SS, Wasantha PLP, Ranjith PG et al (2014) Effect of cooling rate on the mechanical behavior of heated Strathbogie granite with different grain sizes. Int J Rock Mech Min Sci 70:381–387. https://doi.org/10.1016/j.ijrmms.2014.04.003

Shen YJ, Hou X, Yuan JQ et al (2020) Thermal deterioration of high-temperature granite after cooling shock: multiple-identification and damage mechanism. Bull Eng Geol Environ 79(10):5385–5398. https://doi.org/10.1007/s10064-020-01888-7

Siegesmund S, Ullemeyer K, Weiss T et al (2000) Physical weathering of marbles caused by anisotropic thermal expansion. Int J Earth Sci 89(1):170–182. https://doi.org/10.1007/s005310050324

Sun Q, Zhang WQ, Xue L et al (2015) Thermal damage pattern and thresholds of granite. Environ Earth Sci 74:2341–2349. https://doi.org/10.1007/s12665-015-4234-9

Tang S, Wang J, Chen P (2020) Theoretical and numerical studies of cryogenic fracturing induced by thermal shock for reservoir stimulation. Int J Rock Mech Min Sci 125:104160. https://doi.org/10.1016/j.ijrmms.2019.104160

Tischner T, Schindler M, Jung R et al (2007) HDR project Soultz: hydraulic and seismic observations during stimulation of the 3 deep wells by massive water injections. In: Proceedings, 32nd workshop on Geothermal Engineering, Stanford University, Stanford, California 22–24

Tran NH, Rahman SS (2007) Development of hot dry rocks by hydraulic stimulation: natural fracture network simulation. Theor Appl Fract Mech 47(1):77–85. https://doi.org/10.1016/j.tafmec.2006.10.007

Ueda A, Nakatsuka Y, Kunieda M et al (2009) Laboratory and field tests of CO_2—water injection into the Ogachi hot dry rock site, Japan. Energy Procedia 1(1):3669–3674. https://doi.org/10.1016/j.egypro.2009.02.164

Vázquez P, Shushakova V, Gómez-Heras M (2015) Influence of mineralogy on granite decay induced by temperature increase: experimental observations and stress simulation. Eng Geol 189:58–67. https://doi.org/10.1016/j.enggeo.2015.01.026

Wang F, Konietzky H, Frühwirt T et al (2020) Laboratory testing and numerical simulation of properties and thermal-induced cracking of Eibenstock granite at elevated temperatures. Acta Geotech 15:2259–2275. https://doi.org/10.1007/2Fs11440-020-00926-8

Wong LNY, Li ZH, Kang HM et al (2017) Dynamic loading of Carrara Marble in a heated state. Rock Mech Rock Eng 50:1487–1505. https://doi.org/10.1007/s00603-017-1170-x

Wu QH, Weng L, Zhao YL et al (2019) On the tensile mechanical characteristics of fine-grained granite after heating/cooling treatments with different cooling rates. Eng Geol 253:94–110. https://doi.org/10.1016/j.enggeo.2019.03.014

Yang SQ, Ranjith PG, Jing HW et al (2017) An experimental investigation on thermal damage and failure mechanical behavior of granite after exposure to different high temperature treatments. Geothermics 65:180–197. https://doi.org/10.1016/j.geothermics.2016.09.008

Ye JH, Wu FQ, Sun JZ (2009) Estimation of the tensile elastic modulus using Brazilian disc by applying diametrically opposed concentrated loads. Int J Rock Mech Min Sci 46:568–576. https://doi.org/10.1016/j.ijrmms.2008.08.004

Yin TB, Li XB, Cao WZ et al (2015) Effects of thermal treatment on tensile strength of Laurentian granite using Brazilian test. Rock Mech Rock Eng 48:2213–2223. https://doi.org/10.1007/s00603-015-0712-3

Yin TB, Shu RH, Li XB (2016) Comparison of mechanical properties in high temperature and thermal treatment granite. Trans Nonferrous Met Soc China 26(7):1926–1937. https://doi.org/10.1016/S1003-6326(16)64311-X

Yu CB, Ji SC, Li Q (2016) Effects of porosity on seismic velocities, elastic moduli and Poisson's ratios of solid materials and rocks. J Rock Mech Geotech Eng 8(1):35–49. https://doi.org/10.1016/j.jrmge.2015.07.004

Yu QL, Ranjith PG, Liu HY et al (2015) A mesostructure-based damage model for thermal cracking analysis and application in granite at elevated temperatures. Rock Mech Rock Eng 48(6):2263–2282. https://doi.org/10.1007/s00603-014-0679-5

Zeng YC, Su Z, Wu NY (2013) Numerical simulation of heat production potential from hot dry rock by water circulating through two horizontal wells at Desert Peak geothermal field. Energy 56:92–107. https://doi.org/10.1016/j.energy.2013.04.055

Zhang F, Zhao JJ, Hu DW et al (2018a) Evolution of bulk compressibility and permeability of granite due to thermal cracking. Geotechnique 69(10):1–11. https://doi.org/10.1680/jgeot.18.P.005

Zhang F, Zhao JJ, Hu DW et al (2018b) Laboratory investigation on physical and mechanical properties of granite after heating and water-cooling treatment. Rock Mech Rock Eng 51(3):677–694. https://doi.org/10.1007/s00603-017-1350-8

Zhang F, Zhang YH, Hu DW et al (2021) Modification of poroelastic properties in granite by heating–cooling treatment. Acta Geotech. https://doi.org/10.1007/s11440-021-01163-3

Zhang F, Zhang YH, Yu YD, Hu DW, Shao JF (2020a) Influence of cooling rate on thermal degradation of physical and mechanical properties of granite. Int J Rock Mech Min Sci 129:104285. https://doi.org/10.1016/j.ijrmms.2020.104285

Zhang HY, Gao DL, Salehi S et al (2014) Effect of fluid temperature on rock failure in borehole drilling. J Eng Mech 140(1):82–90. https://doi.org/10.1061/(ASCE)EM.1943-7889.0000648

Zhang WQ, Sun Q, Hao SQ et al (2016) Experimental study on the variation of physical and mechanical properties of rock after high temperature treatment. Appl Therm Eng 98:1297–1304. https://doi.org/10.1016/j.applthermaleng.2016.01.010

Zhang Z, Ma B , Ranjith P G et al (2020b) Indications of risks in geothermal systems caused by changes in pore structure and mechanical properties of granite: an experimental study. Bull Eng Geol Environ 79:5399–5414. https://doi.org/10.1007/s10064-020-01901-z

Zhao ZH (2015) Thermal influence on mechanical properties of granite: a microcracking perspective. Rock Mech Rock Eng 49:747–762. https://doi.org/10.1007/s00603-015-0767-1

Zhao ZH, Xu HR, Wang J et al (2020) Auxetic behavior of Beishan granite after thermal treatment: a microcracking perspective. Eng Fract Mech 231:107017. https://doi.org/10.1016/j.engfracmech.2020.107017

Zhu D, Jing HW, Yin Q, Ding SX, Zhang JH (2020a) Mechanical characteristics of granite after heating and water-cooling cycles. Rock Mech Rock Eng 53(4):2015–2025. https://doi.org/10.1007/s00603-019-01991-6

Zhu ZN, Tian H, Chen J, Jiang GS, Dou B, Xiao P, Mei G (2020b) Experimental investigation of thermal cycling effect on physical and mechanical properties of heated granite after water cooling. Bull Eng Geol Environ 79(5):2457–2465. https://doi.org/10.1007/s10064-019-01705-w

Zhu ZN, Tian H, Mei G et al (2021) Experimental investigation on mechanical behaviors of Nanan granite after thermal treatment under conventional triaxial compression. Environ Earth Sci 80:46. https://doi.org/10.1007/s12665-020-09326-3

Ziagos J, Phillips BR, Boyd L et al (2013) A technology roadmap for strategic development of enhanced geothermal systems. In: Proceedings of the 38th Workshop on Geothermal Reservoir Engineering, Stanford, CA, 2013. Citeseer, pp 11–13